Electronic Supplementary Material (ESI) for Journal of Materials Chemistry A.

Near Infrared Electron Acceptors with Photoresponse Beyond 1000 nm for Highly Efficient Organic Solar Cells

Chengliang He,[†a] Yaokai Li,[†a] Yanfeng Liu,[b] Yuhao Li,[c] Guanqing Zhou,[d] Shuixing Li,[a] Haiming Zhu,[e] Xinhui Lu,[c] Fengling Zhang,[b] Chang-Zhi Li,*[a] and Hongzheng Chen*[a]

[a] State Key Laboratory of Silicon Materials, MOE Key Laboratory of Macromolecular Synthesis and Functionalization, Department of Polymer Science and Engineering, Zhejiang University, Hangzhou 310027, P.R. China.

[b] Department of Physics, Chemistry and Biology (IFM), Linköping University, Linköping 581 83, Sweden.

[c] Department of Physics, The Chinese University of Hong Kong, New Territories, Hong Kong 999077, P.R. China.

[d] School of Chemistry and Chemical Engineering Center for Advanced Electronic Materials and Devices, Shanghai Jiao Tong University, Shanghai 200240, P. R. China.

[e] Department of Chemistry, Zhejiang University, Hangzhou 310027, P.R. China.

[†] C. He and Y. Li contributed equally to this work.

*E-mail: hzchen@zju.edu.cn (H. Chen), czli@zju.edu.cn (C.-Z. Li).

—**Experimental Section**

—**Device Fabrication and Characterization**

—**Experimental Data**

Experimental Section

Materials

All reagents and solvents, unless otherwise specified, were purchased from commercial sources and were used without further purification.

Routine Characterization

^{1}H NMR and ^{13}C NMR tests were carried out with an Agilent DD2 600 (600 MHz) nuclear magnetic resonance (NMR) spectroscope and a Bruker Advance III 400 (400 MHz) NMR spectroscope. Matrix-assisted laser desorption/ionization time of flight (MALDI-TOF) MS spectrum were obtained on the Bruker Ultraflex MALDI. Cyclic voltammetry (CV) was done on a CHI600A electrochemical workstation by utilizing the acetonitrile solution of 0.1 mol/L tetrabutylammoniumhexafluorophosphate (Bu_4NPF_6). The CV curves were recorded versus the potential of SCE, which was calibrated by the ferrocene-ferrocenium (Fc/Fc^+) redox couple (4.8 eV below the vacuum level). Then LUMO and HOMO levels was calculated by the equation of $E_{\mathrm{LUMO/HOMO}}$ = -e ($E_{\mathrm{red/ox}}$+4.41) (eV). UV-vis absorption spectra were measured on a Shimadzu UV-1800 spectrophotometer.

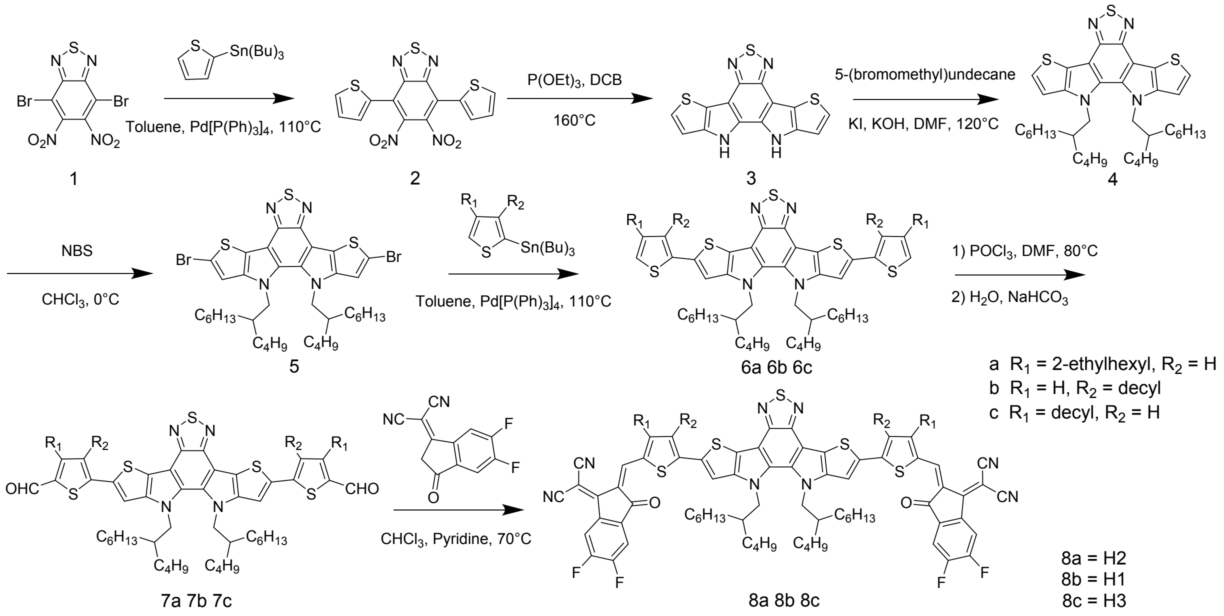

Synthesis of H1, H2 and H3

Scheme S1. Synthetic route of H1, H2 and H3.

5,6-dinitro-4,7-di(thiophen-2-yl)benzo[c][1,2,5]thiadiazole (**2**)

4,7-dibromo-5,6-dinitrobenzo[c][1,2,5]thiadiazole (2.00 g, 5.21 mmol) and tributyl(thiophen-2-yl)stannane (4.18 g, 11.20 mmol) were dissolved into the solution of Toulene (40 mL) and N, N-dimethylformamide (DMF, 4 mL), then the mixture was frozen by liquid nitrogen, after vacuum and Ar circulated for three times, add the Pd(PPh$_3$)$_4$ (0.06 g, 0.051 mmol) in, followed by another three times of the former circulation. The mixture was refluxed at 110 °C for 24 h. Using water to wash the crude product and dichloromethane to obtain the organic phase. After removing the solvent, silica gel column chromatography was used to purify the product with the mixture of

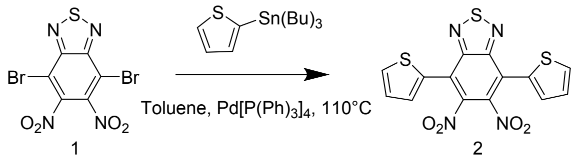

petroleum ether and dichloromethane (1:2~1:4, v/v) as the eluent, yielding an orange solid (1.87 g, 92%). ^{1}H NMR (400 MHz, CDCl$_3$, δ): 7.75 (d, *J* = 5.0 Hz, 2H), 7.52 (d, *J* = 2.9 Hz, 2H), 7.25 (t, *J* = 3.9 Hz, 2H).

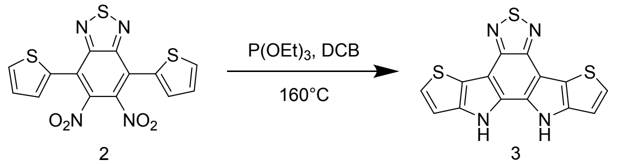

10,11-dihydro-[1,2,5]thiadiazolo[3,4-e]thieno[2',3':4,5]pyrrolo[3,2-g]thieno[3,2-b]indole (**3**)

To a Schlenk tube under Ar atmosphere, compound **2** (1.87 g, 4.78 mmol) combined with *o*-dichlorobenzene (10 mL) and triethyl phosphite (14 mL) were added successively. After being refluxed at 160 °C overnight, the reaction system was cooled and then concentrated under high vacuum, the resulting product was collected as mixture and used as compound in the next step without further purification.

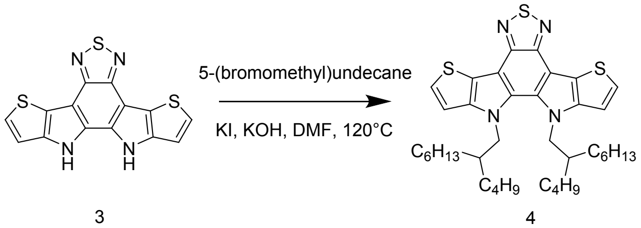

10,11-bis(2-butyloctyl)-10,11-dihydro-[1,2,5]thiadiazolo[3,4-e]thieno[2',3':4,5]pyrrolo[3,2-g]thieno[3,2-b]indole (**4**)

Compound **3** obtained from the former step was dissolved in DMF (40 mL), then 5-(bromomethyl)undecane (4.76 g, 19.12 mmol), potassium hydroxide (2.68 g, 47.8 mmol) and potassium iodide (50 mg) were added. The reaction mixture was deoxygenated with Ar for 0.5 h, then refluxed at 120 °C for 24 h. After pouring into water, the resulting mixture was extracted with dichloromethane. After removing the solvent, silica gel column chromatography was used to purify the product with the mixture of petroleum ether and dichloromethane (5:1, v/v) as the eluent, yielding a dark yellow oil (1.20 g, 1.82 mmol). From compound 2 to compound 4, the total yield is 38%. ^{1}H NMR (400 MHz, $CDCl_3$, δ): 7.43 (d, *J* = 5.2 Hz, 2H), 7.17 (d, *J* = 5.2 Hz, 2H), 4.50 (d, *J* = 7.7 Hz, 4H), 2.04-1.96 (m, 2H), 1.04-0.84 (m, 28H), 0.77-0.58 (m, 16H).

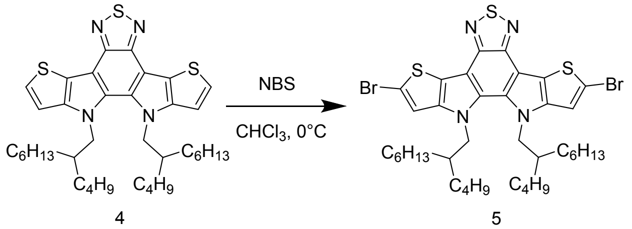

2,8-dibromo-10,11-bis(2-butyloctyl)-10,11-dihydro-[1,2,5]thiadiazolo[3,4-e]thieno[2',3':4,5]pyrrolo[3,2-g]thieno[3,2-b]indole (**5**)

Compound **4** (1.20 g, 1.82 mmol) was dissolved in 20 mL chloroform ($CHCl_3$) in dark, then N-Bromosuccinimide (0.66 g, 3.73 mmol) was divided into 5 parts on average and added to reaction system every 20 min. After being stirred for 2 h at room temperature, the mixture was then quenched with water, extracted with dichloromethane, and purified by silica gel chromatography with the mixture of petroleum ether and dichloromethane (3:1, v/v) as eluent to yield the compound as orange oil (1.25 g, 84%). ^{1}H NMR (400 MHz, $CDCl_3$, δ): 7.19 (s, 2H), 4.41 (d, *J* = 7.6 Hz, 4H), 1.99-1.90 (m, 2H), 1.06-0.84 (m, 28H), 0.77-0.62 (m, 16H).

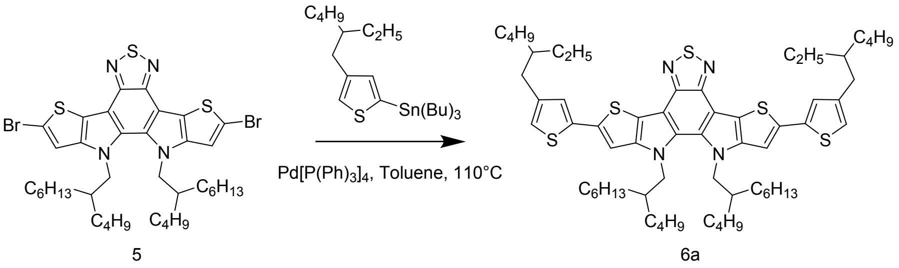

10,11-bis(2-butyloctyl)-2,8-bis(4-(2-ethylhexyl)thiophen-2-yl)-10,11-dihydro-[1,2,5]thiadiazolo[3,4-e]thieno[2',3':4,5]pyrrolo[3,2-g]thieno[3,2-b]indole (**6a**)

Compound **5** (0.20 g, 0.24 mmol) and tributyl(4-(2-ethylhexyl)thiophen-2-yl)stannane (0.24 g, 0.50 mmol) were dissolved into the solution of Toulene (20 mL) and N, N-dimethylformamide (DMF, 2 mL), then the mixture was frozen by liquid nitrogen, after vacuum and Ar circulated for three times, add the $Pd(PPh_3)_4$ (0.04 g, 0.034 mmol) in, followed by another three times of the former circulation. The mixture was refluxed at 110 °C for 24 h. Using water to wash the crude product and dichloromethane to obtain the organic phase. After removing the solvent, silica gel column chromatography was used to purify the product with the mixture of petroleum ether and dichloromethane (5:1~3:1, v/v) as the eluent, yielding a red oil (0.21 g, 82%). ^{1}H NMR (600 MHz, $CDCl_3$, δ): 7.20 (s, 2H), 7.11 (s, 2H), 6.82 (s, 2H), 4.46 (d, *J* = 4.3 Hz, 4H), 2.57 (d, *J* = 4.4 Hz, 4H), 2.07-2.00 (m, 2H), 1.64-1.58 (m, 2H), 1.36-1.25 (m, 20H), 1.02-0.83 (m, 40H), 0.73-0.63 (m, 12H).

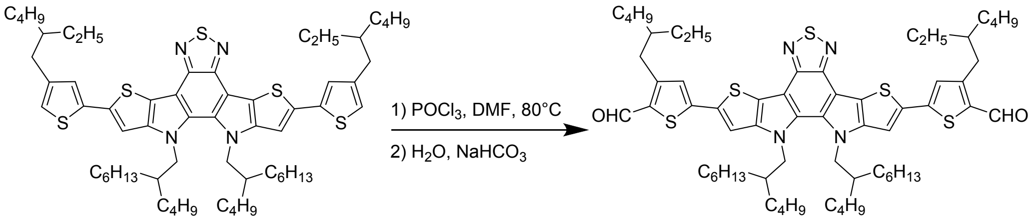

6a

7a

5,5'-(10,11-bis(2-butyloctyl)-10,11-dihydro-[1,2,5]thiadiazolo[3,4-e]thieno[2',3':4,5]pyrrolo[3,2-g]thieno[3,2-b]indole-2,8-diyl)bis(3-(2-ethylhexyl)thiophene-2-carbaldehyde) (**7a**)

To a Schlenk tube under Ar atmosphere at 0 °C, 1 mL DMF and 0.8 mL $POCl_3$ were injected successively. After being stirred for 0.5 h at 0 °C, compound **6a** (0.21 g, 0.20 mmol) was added into the reaction system through 1,2-dichloroethane (15 mL) as the solvent. The mixture was refluxed at 80 °C for 8 h. After cooling to r.t., the mixture was extracted with a syringe and injected into a $NaHCO_3$ aqueous solution dropwise, then stirred for another 8 h. Using water to wash the crude product and dichloromethane to obtain the organic phase. After removing the solvent, silica gel column chromatography was used to purify the product with the mixture of petroleum ether and dichloromethane (2:3~1:4, v/v) as the eluent, yielding a red solid (0.17 g, 76%). ^{1}H NMR (400 MHz, $CDCl_3$, δ): 10.01 (s, 2H), 7.41 (s, 2H), 7.16 (s, 2H), 4.50 (d, *J* = 7.2 Hz, 4H), 2.90 (d, *J* = 7.2 Hz, 4H), 2.08-1.97 (m, 2H), 1.80-1.70 (m, 2H), 1.42-1.19 (m, 20H), 1.12-0.82 (m, 40H), 0.73-0.63 (m, 12H).

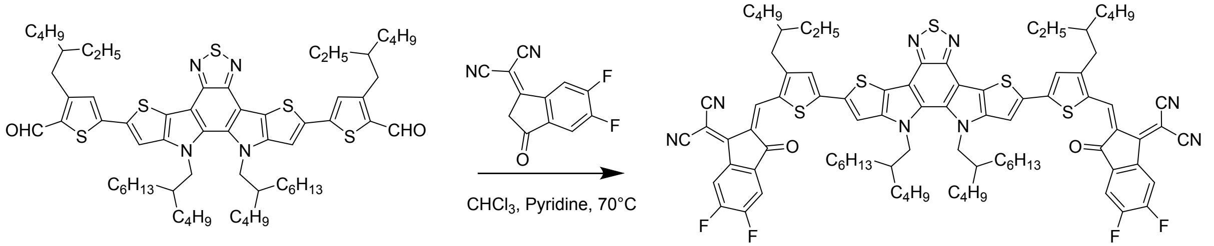

7a

8a

2,2'-((2Z,2'Z)-(((10,11-bis(2-butyloctyl)-10,11-dihydro-[1,2,5]thiadiazolo[3,4-e]thieno[2',3':4,5]pyrrolo[3,2-g]thieno[3,2-b]indole-2,8-diyl)bis(3-(2-ethylhexyl)thiophene-5,2-diyl))bis(methanylylidene))bis(5,6-difluoro-3-oxo-2,3-dihydro-1H-indene-2,1-diylidene))dimalononitrile (**8a**)

To a Schlenk tube were added compound **7a** (0.16 g, 0.14 mmol), 2-(5,6-difluoro-3-oxo-2,3-dihydro-1H-inden-1-ylidene)malononitrile (0.13 g, 0.58 mmol) and dried $CHCl_3$ (40mL). Then the mixture was frozen by liquid nitrogen, after vacuum and Ar circulated for three times, 0.5 mL pyridine was added. The mixture was refluxed at 70 °C for 24 h. After removing the solvent, silica gel column chromatography was used to purify the product with the mixture of petroleum ether and dichloromethane (1:1~1:2, v/v) as the eluent, yielding a black solid (0.17 g, 80%). ^{1}H NMR (400 MHz, $CDCl_3$, δ): 8.98 (s, 2H), 8.56 (q, *J* = 6.5 Hz, 2H), 7.73-7.62 (m, 4H), 7.33 (s, 2H), 4.56

(d, J = 7.2 Hz, 4H), 2.95 (d, J = 7.2 Hz, 4H), 2.18-2.04 (m, 2H), 1.81-1.67 (m, 2H), 1.46-1.23 (m, 20H), 1.14-0.87 (m, 40H), 0.76-0.66 (m, 12H). MS (MALDI-TOF): Calcd for $C_{88}H_{94}F_4N_8O_2S_5$ (M^+): 1532.07, Found: 1531.34.

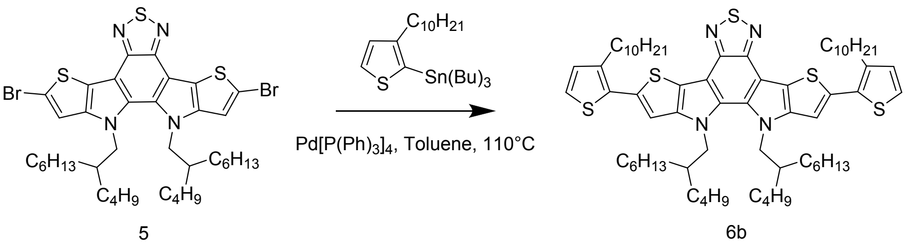

10,11-bis(2-butyloctyl)-2,8-bis(3-decylthiophen-2-yl)-10,11-dihydro-[1,2,5]thiadiazolo[3,4-e]thieno[2',3':4,5]pyrrolo[3,2-g]thieno[3,2-b]indole (**6b**)

Compound **5** (0.20 g, 0.24 mmol) and tributyl(3-decylthiophen-2-yl)stannane (0.26 g, 0.50 mmol) were dissolved into the solution of Toulene (20 mL) and N, N-dimethylformamide (DMF, 2 mL), then the mixture was frozen by liquid nitrogen, after vacuum and Ar circulated for three times, add the $Pd(PPh_3)_4$ (0.04 g, 0.034 mmol) in, followed by another three times of the former circulation. The mixture was refluxed at 110 °C for 24 h. Using water to wash the crude product and dichloromethane to obtain the organic phase. After removing the solvent, silica gel column chromatography was used to purify the product with the mixture of petroleum ether and dichloromethane (5:1~4:1, v/v) as the eluent, yielding a red oil (0.20 g, 75%). ^1H NMR (400 MHz, $CDCl_3$, δ): 7.24 (d, J = 5.2 Hz, 2H), 7.18 (s, 2H), 7.01 (d, J = 5.2 Hz, 2H), 4.50 (d, J = 7.6 Hz,

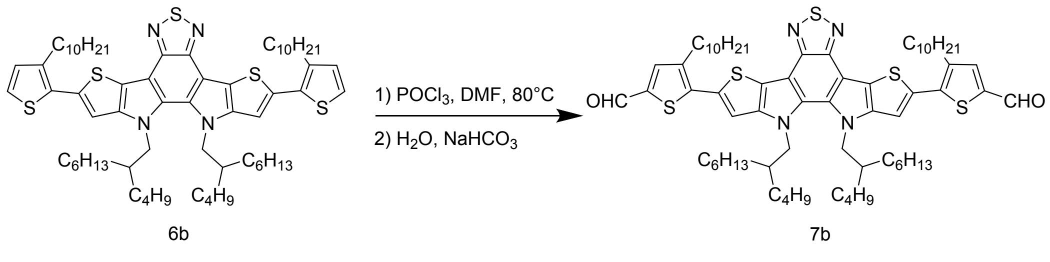

4H), 2.93 (t, $J = 7.7$ Hz, 4H), 2.10-2.00 (m, 2H), 1.77-1.66 (m, 4H), 1.43-1.22 (m, 32H), 1.09-0.84 (m, 34H), 0.74-0.64 (m, 12H).

5,5'-(10,11-bis(2-butyloctyl)-10,11-dihydro-[1,2,5]thiadiazolo[3,4-e]thieno[2',3':4,5]pyrrolo[3,2-g]thieno[3,2-b]indole-2,8-diyl)bis(4-decylthiophene-2-carbaldehyde) (**7b**)

To a Schlenk tube under Ar atmosphere at 0 °C, 1 mL DMF and 0.8 mL $POCl_3$ were injected successively. After being stirred for 0.5 h at 0 °C, compound **6b** (0.20 g, 0.18 mmol) was added into the reaction system through 1,2-dichloroethane (15 mL) as the solvent. The mixture was refluxed at 80 °C for 8 h. After cooling to r.t., the mixture was extracted with a syringe and injected into a $NaHCO_3$ aqueous solution dropwise, then stirred for another 8 h. Using water to wash the crude product and dichloromethane to obtain the organic phase. After removing the solvent, silica gel column chromatography was used to purify the product with the mixture of petroleum ether and dichloromethane (2:3~1:3, v/v) as the eluent, yielding a red solid (0.17 g, 80%). ^1H NMR (400 MHz, $CDCl_3$, δ): 9.87 (s, 2H), 7.66 (s, 2H), 7.38 (s, 2H), 4.52 (d, $J = 7.6$ Hz, 4H), 3.00 (t, $J = 7.7$ Hz, 4H), 2.08-1.98 (m, 2H), 1.82-1.72 (m, 4H), 1.43-1.23 (m, 32H), 1.09-0.84 (m, 34H), 0.72-0.63 (m, 12H).

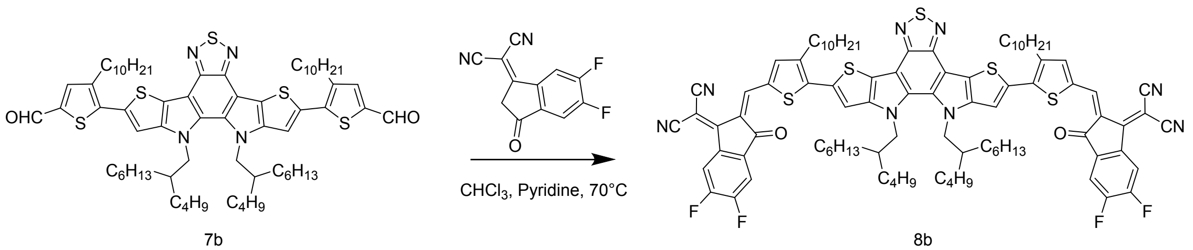

2,2'-((2Z,2'Z)-(((10,11-bis(2-butyloctyl)-10,11-dihydro-[1,2,5]thiadiazolo[3,4-e]thieno[2',3':4,5]pyrrolo[3,2-g]thieno[3,2-b]indole-2,8-diyl)bis(4-decylthiophene-5,2-

diyl))bis(methanylylidene))bis(5,6-difluoro-3-oxo-2,3-dihydro-1H-indene-2,1-diylidene))dimalononitrile (**8b**)

To a Schlenk tube were added compound **7b** (0.16 g, 0.14 mmol), 2-(5,6-difluoro-3-oxo-2,3-dihydro-1H-inden-1-ylidene)malononitrile (0.13 g, 0.58 mmol) and dried $CHCl_3$ (40mL). Then the mixture was frozen by liquid nitrogen, after vacuum and Ar circulated for three times, 0.5 mL pyridine was added. The mixture was refluxed at 70 °C for 24 h. After removing the solvent, silica gel column chromatography was used to purify the product with the mixture of petroleum ether and dichloromethane (1:1~1:3, v/v) as the eluent, yielding a black solid (0.18 g, 83%). ^1H NMR (600 MHz, $CDCl_3$, δ): 8.78 (s, 2H), 8.57-8.46 (m, 2H), 7.79-7.53 (m, 6H), 4.58 (s, 4H), 3.01 (s, 4H), 2.12 (s, 2H), 1.85-1.79 (m, 4H), 1.53-1.49 (m, 4H), 1.43-1.38 (m, 4H), 1.36-1.24 (m, 20H), 1.16-0.93 (m, 28H), 0.90-0.80 (m, 10H), 0.74-0.68 (m, 12H). MS (MALDI-TOF): Calcd for $C_{92}H_{102}F_4N_8O_2S_5$ (M^+): 1588.18, Found: 1588.40.

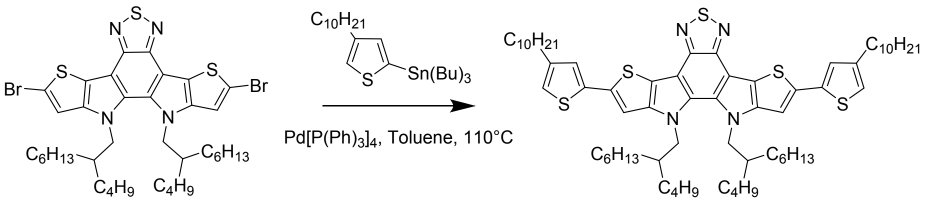

5

6c

10,11-bis(2-butyloctyl)-2,8-bis(4-decylthiophen-2-yl)-10,11-dihydro-[1,2,5]thiadiazolo[3,4-e]thieno[2',3':4,5]pyrrolo[3,2-g]thieno[3,2-b]indole (**6c**)

Compound **5** (0.40 g, 0.49 mmol) and tributyl(4-decylthiophen-2-yl)stannane (0.52 g, 1.02 mmol) were dissolved into the solution of Toulene (30 mL) and N, N-dimethylformamide (DMF, 3 mL), then the mixture was frozen by liquid nitrogen, after vacuum and Ar circulated for three times, add the $Pd(PPh_3)_4$ (0.05 g, 0.042 mmol) in, followed by another three times of the former circulation.

The mixture was refluxed at 110 °C for 24 h. Using water to wash the crude product and dichloromethane to obtain the organic phase. After removing the solvent, silica gel column chromatography was used to purify the product with the mixture of petroleum ether and dichloromethane (5:1~4:1, v/v) as the eluent, yielding a red oil (0.49 g, 91%). ^{1}H NMR (400 MHz, $CDCl_3$, δ): 7.20 (s, 2H), 7.14 (s, 2H), 6.85 (s, 2H), 4.46 (d, *J* = 7.6 Hz, 4H), 2.64 (t, *J* = 7.5 Hz, 4H), 2.07-1.99 (m, 2H), 1.71-1.63 (m, 4H), 1.40-1.24 (m, 32H), 1.10-0.84 (m, 34H), 0.73-0.63 (m, 12H).

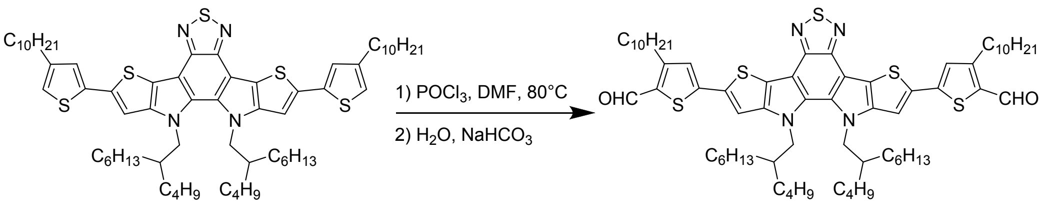

6c 7c

5,5'-(10,11-bis(2-butyloctyl)-10,11-dihydro-[1,2,5]thiadiazolo[3,4-e]thieno[2',3':4,5]pyrrolo[3,2-g]thieno[3,2-b]indole-2,8-diyl)bis(3-decylthiophene-2-carbaldehyde) (**7c**)

To a Schlenk tube under Ar atmosphere at 0 °C, 1 mL DMF and 0.8 mL $POCl_3$ were injected successively. After being stirred for 0.5 h at 0 °C, compound **6c** (0.48 g, 0.43 mmol) was added into the reaction system through 1,2-dichloroethane (15 mL) as the solvent. The mixture was refluxed at 80 °C for 8 h. After cooling to r.t., the mixture was extracted with a syringe and injected into a $NaHCO_3$ aqueous solution dropwise, then stirred for another 8 h. Using water to wash the crude product and dichloromethane to obtain the organic phase. After removing the solvent, silica gel column chromatography was used to purify the product with the mixture of petroleum ether and dichloromethane (2:3~1:4, v/v) as the eluent, yielding a red solid (0.42 g, 84%). ^{1}H NMR (400 MHz, $CDCl_3$, δ): 10.02 (s, 2H), 7.40 (s, 2H), 7.19 (s, 2H), 4.50 (d, *J* = 7.2 Hz, 4H), 2.99 (t, *J* = 7.5

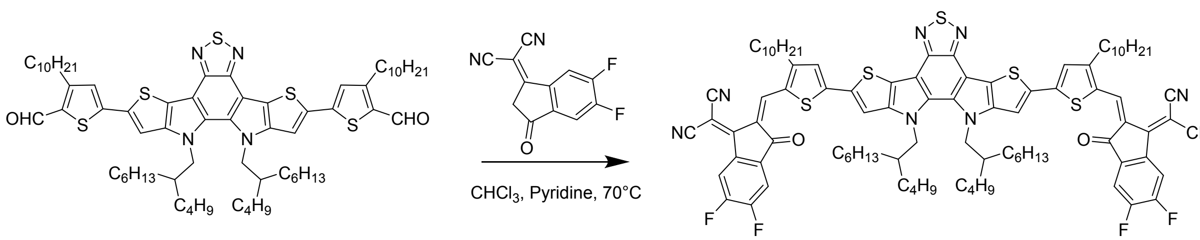

7c 8c

Hz, 4H), 2.06-1.98 (m, 2H), 1.79-1.69 (m, 4H), 1.45-1.23 (m, 32H), 1.12-0.83 (m, 34H), 0.72-0.63 (m, 12H).

2,2'-((2Z,2'Z)-(((10,11-bis(2-butyloctyl)-10,11-dihydro-[1,2,5]thiadiazolo[3,4-e]thieno[2',3':4,5]pyrrolo[3,2-g]thieno[3,2-b]indole-2,8-diyl)bis(3-decylthiophene-5,2-diyl))bis(methanylylidene))bis(5,6-difluoro-3-oxo-2,3-dihydro-1H-indene-2,1-diylidene))dimalononitrile (**8c**)

To a Schlenk tube were added compound **7c** (0.42 g, 0.36 mmol), 2-(5,6-difluoro-3-oxo-2,3-dihydro-1H-inden-1-ylidene)malononitrile (0.33 g, 1.44 mmol) and dried $CHCl_3$ (50mL). Then the mixture was frozen by liquid nitrogen, after vacuum and Ar circulated for three times, 0.5 mL pyridine was added. The mixture was refluxed at 70 °C for 24 h. After removing the solvent, silica gel column chromatography was used to purify the product with the mixture of petroleum ether and dichloromethane (1:1~1:3, v/v) as the eluent, yielding a black solid (0.46 g, 80%). ^{1}H NMR (400 MHz, $CDCl_3$, δ): 8.95 (s, 2H), 8.52 (q, J = 6.5 Hz, 2H), 7.69 (t, J = 7.6 Hz, 2H), 7.60 (s, 2H), 7.31 (s, 2H), 4.56 (d, J = 7.2 Hz, 4H), 3.00 (t, J = 7.6 Hz, 4H), 2.23-2.08 (m, 2H), 1.82-1.66 (m, 4H), 1.51-1.42 (m, 4H), 1.39-1.25 (m, 24H), 1.20-0.95 (m, 28H), 0.92-0.82 (m, 10H), 0.77-0.68 (m, 12H). MS (MALDI-TOF): Calcd for $C_{92}H_{102}F_4N_8O_2S_5$ (M^+): 1588.18, Found: 1587.42.

Device Fabrication and Characterization

Device Fabrication

Organic solar cells fabricated on glass substrates commercially pre-coated with a layer of indium tin oxide (ITO), constructing the inverted structure of ITO/ZnO/Active Layer/MoO_3/Ag. Before fabrication, the substrates were pre-cleaned by an ultrasonic bath of detergent, deionized water, acetone and isopropanol consecutively, and then treated in an ultraviolet ozone generator for 15 min. After that, a thin layer ZnO (prepared by using a precursor solution of zinc acetate in 2-methoxyethanol and ethanolamine) was spin coated onto the substrates at 3500 rpm for 60 s and annealed at 170 °C for 20 min. Put the substrates into glovebox, the active layer was spin coated from 17 mg/mL (PBDB-T:acceptor = 1:1.2, 0.5% CN) chloroform solution at 2500 rpm for 30 s. Then an extra pre-annealing at 150 °C for 10 min was carried out. Finally, a layer of MoO_3 (8 nm) and Ag (100 nm) electrode were deposited by thermal evaporation, the devices were completed with an active area of 6 mm^2.

J-V and EQE Measurement

The current density-voltage (*J-V*) curves of OSCs were performed on a Enlitech SS-F5-3A solar simulator under the condition of AM 1.5 G illumination, whose light intensity was calibrated by a standard Si solar cell at 100 mV cm^{-2}. The EQE data were measured by a Solar Cell Spectral Response Measurement System (RE-R, Enlitech).

Electroluminescence Measurement

An external current/voltage source was utilized to provide an external electric field to the pristine and blended solar cells. The electroluminescence emissions were recorded with an Andor spectrometer.

FTPS-EQE Measurement

The FTPS-EQE was measured with a Vertex 70 from Bruker Optics, which was equipped with a quartz tungsten halogen lamp, quartz beam-splitter and external detector option. A low-noise current amplifier (SR570) was employed to amplify the photocurrent produced under illumination of the solar cells, with light modulated by the Fourier transform infrared spectroscope (FTIR). The output voltage of the current amplifier was fed back into the external detector port of the FTIR to use the FTIR software to collect the photocurrent spectra.

$\mathrm{EQE}_{\mathrm{EL}}$ Measurement

The $\mathrm{EQE}_{\mathrm{EL}}$ was recorded with an in-house-built system comprising a Hamamatsu silicon photodiode 1010B, Keithley 2400 source meter (for supplying voltages and recording injected currents), and Keithley 485 picoammeter (for measuring the emitted light intensity).

Transient Absorption Spectroscopy (TAS) Measurement

For femtosecond transient absorption spectroscopy, the fundamental output from Yb:KGW laser (1030 nm, 220 fs Gaussian fit, 100 kHz, Light Conversion Ltd) was separated to two light beam. One was introduced to NOPA (ORPHEUS-N, Light Conversion Ltd) to produce a certain wavelength for pump beam (here we use 750 nm), the other was focused onto a YAG plate to generate white light continuum as probe beam. The pump and probe overlapped on the sample at a small angle less than 10°. The transmitted probe light from sample was collected by a linear CCD array. Then we obtained transient differential transmission signals by equation shown below:

$$\frac{\Delta T}{T} = \frac{T_{pump-on} - T_{pump-off}}{T_{pump-off}} \qquad (1)$$

SCLC Measurement

The charge carrier mobilities of the Donor:Acceptor films were measured using the space charge limited current (SCLC) method. Electron-only devices were fabricated in a structure of ITO/ZnO/Active Layer/PFN-Br/Al whereas Hole-only devices utilizing the structure of ITO/PEDOT:PSS/Active Layer/MoO_3/Ag. The device characteristics were extracted by modeling the dark current under forward bias the SCLC expression described by the Mott-Gurney Law:

$$J=\frac{9}{8}\varepsilon_{\mathrm{r}}\varepsilon_0\mu\frac{V^2}{L^3} \qquad (2)$$

Here, $\varepsilon_r \approx 3$ is the average dielectric constant of the blend film, ε_0 is the permittivity of the free space, μ is the carrier mobility, $L \approx 100$ nm is the thickness of the film, and V is the applied voltage.

AFM Characterization

The samples were fabricated same with OSC conditions. Topographic images of the films were obtained on a VeecoMultiMode AFM in the tapping mode using an etched silicon cantilever at a nominal load of ~2 nN, and the scanning rate for a 2.0 μm×2.0 μm image size was 1.5 Hz.

GIWAXS Measurements

GIWAXS data were carried out with a Xeuss 2.0 SAXS/WAXS laboratory beamline using a Cu X-ray source (8.05 keV, 1.54 Å) and Pilatus3R 300K detector. The incidence angle is 0.2°.

Energy Loss Calculation

$$\begin{aligned} E_{\text{loss}} &= E_g - qV_{oc} \\ &= (E_g - qV_{oc}^{SQ}) + (qV_{oc}^{SQ} - qV_{oc}^{rad}) + (qV_{oc}^{rad} - qV_{oc}) \\ &= (E_g - qV_{oc}^{SQ}) + q\Delta V_{oc}^{rad,below\ gap} + q\Delta V_{oc}^{non-rad} \qquad (3) \\ &= \Delta E_1 + \Delta E_2 + \Delta E_3 \end{aligned}$$

The total energy loss (E_{loss}) can be attributed to three parts following Equation below:

where E_{g} is the bandgap, q is the elementary charge, V_{oc}^{SQ} is the maximum voltage based on the Shockley-Queisser limit (SQ limit), V_{oc}^{rad} is the open-circuit voltage when there is only radiative recombination, $\Delta V_{oc}^{rad,below\ gap}$ is the voltage loss of radiative recombination from the absorption below the bandgap and $\Delta V_{oc}^{non-rad}$ is the voltage loss of non-radiative recombination. ΔE_1 is due to radiative recombination from the absorption above the bandgap, ΔE_2 is due to radiative recombination from the absorption below the bandgap and ΔE_3 is due to non-radiative recombination. The third part, non-radiative loss, could be directly calculated by Equation :

$$\Delta E_3 = q\Delta V_{oc}^{non-rad} = -kT\ln(EQE_{EL}) \qquad (4)$$

where k is the Boltzmann constant, T is temperature and EQE_{EL} is radiative quantum efficiency of the OSCs when charge carriers are injected into the device in the dark.

Urbach Energy Calculation

Since the FTPS-EQE method is suitable for highly sensitive absorption measurements and the

$$EQE(E) \propto \alpha(E) \propto e^{\frac{E-E_g}{E_{\text{U}}}} \qquad (5)$$

EQE is direct proportion to the absorbance according to:

the values of E_{U} could be obtained from the FTPS-EQE curves by an exponential fit.

Experimental Data

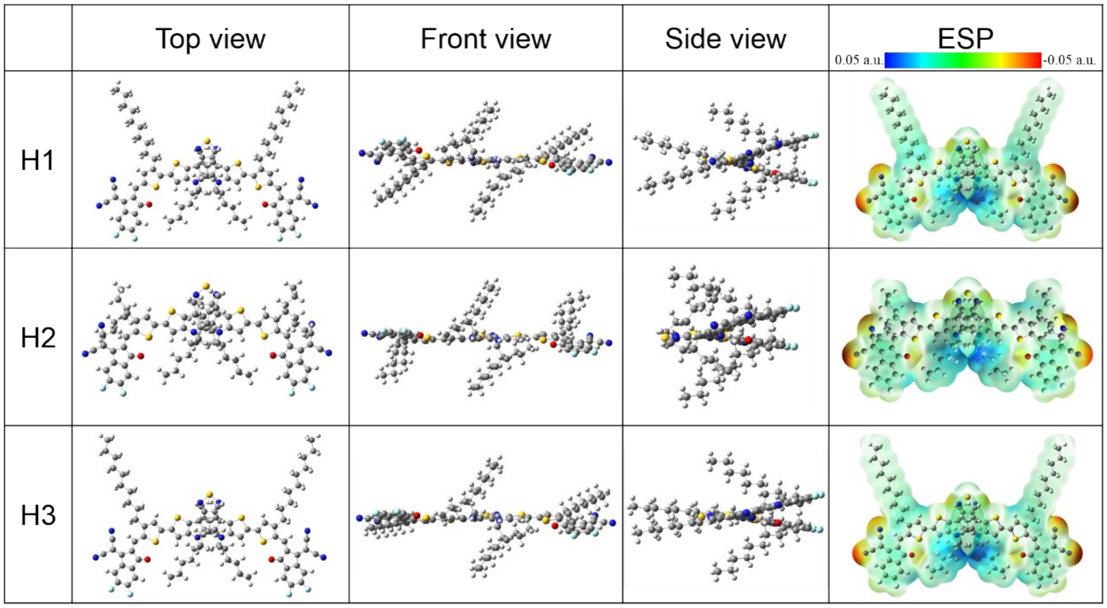

Fig. S1 Results of molecular geometries and isosurfaces of the electrostatic potential of acceptors based on the DFT calculation.

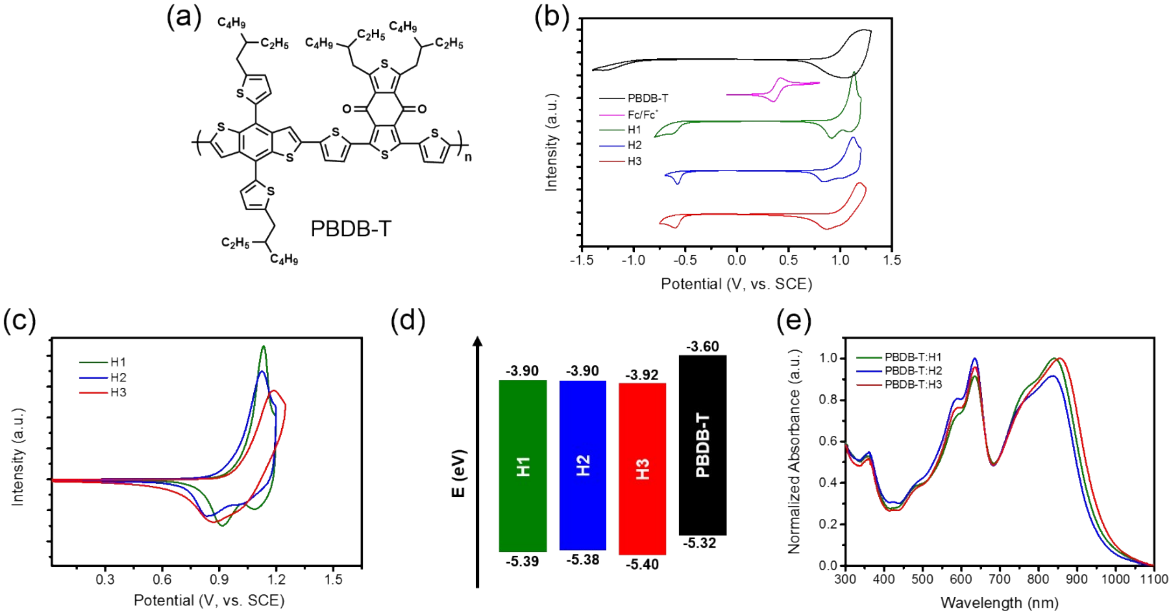

Fig. S2 (a) Chemical structure of PBDB-T. (b) (c) Cyclic voltammograms of PBDB-T and acceptors. (d) Energy-level diagram of PBDB-T, H1, H2 and H3. (e) UV-vis absorption spectra of the three blend films.

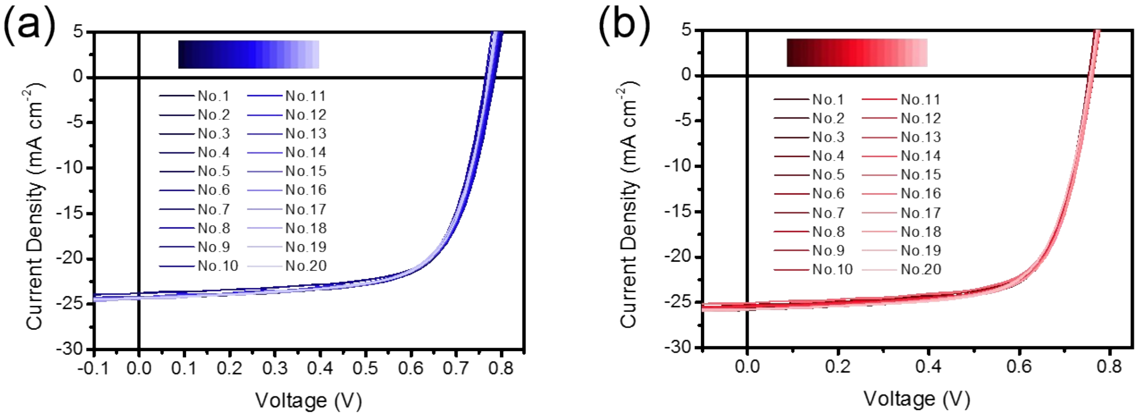

Fig. S3 *J*–*V* curves of 20 independent devices based on (a) PBDB-T:H2 and (b) PBDB-T:H3 blend films.

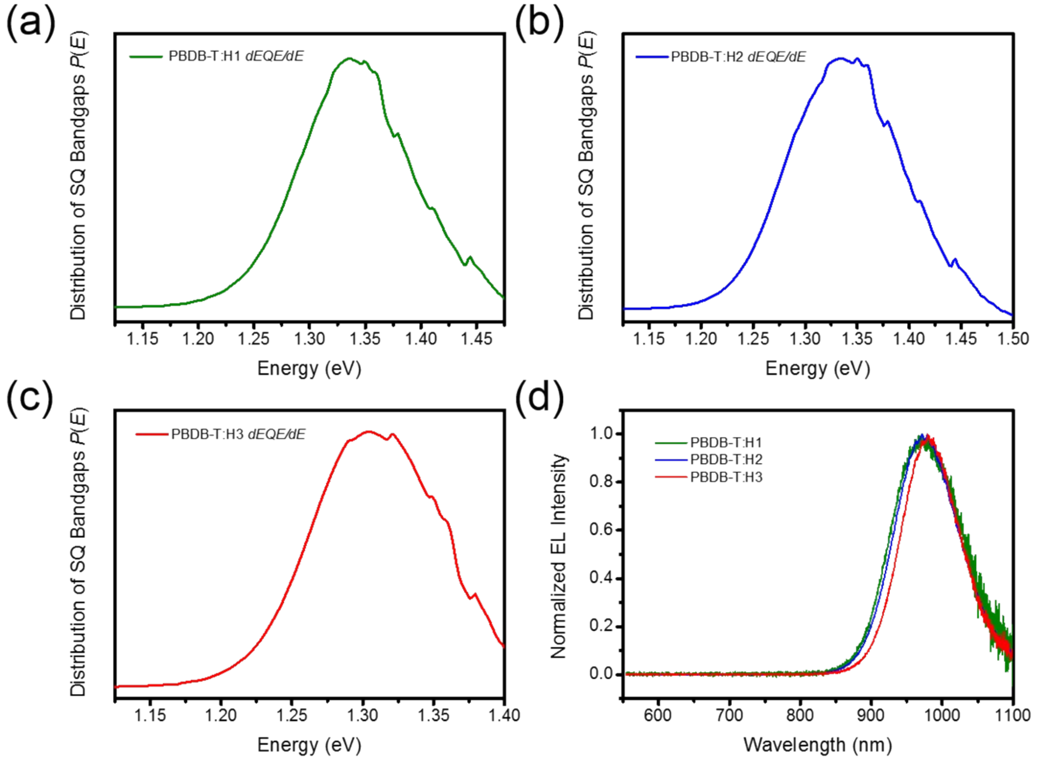

Fig. S4 Distribution of SQ bandgaps *P*(*E*) for (a) PBDB-T:H1, (b) PBDB-T:H2, (c) PBDB-T:H3. (d) Normalized EL spectra of PBDB-T:H1, PBDB-T:H2 and PBDB-T:H3 blend films.

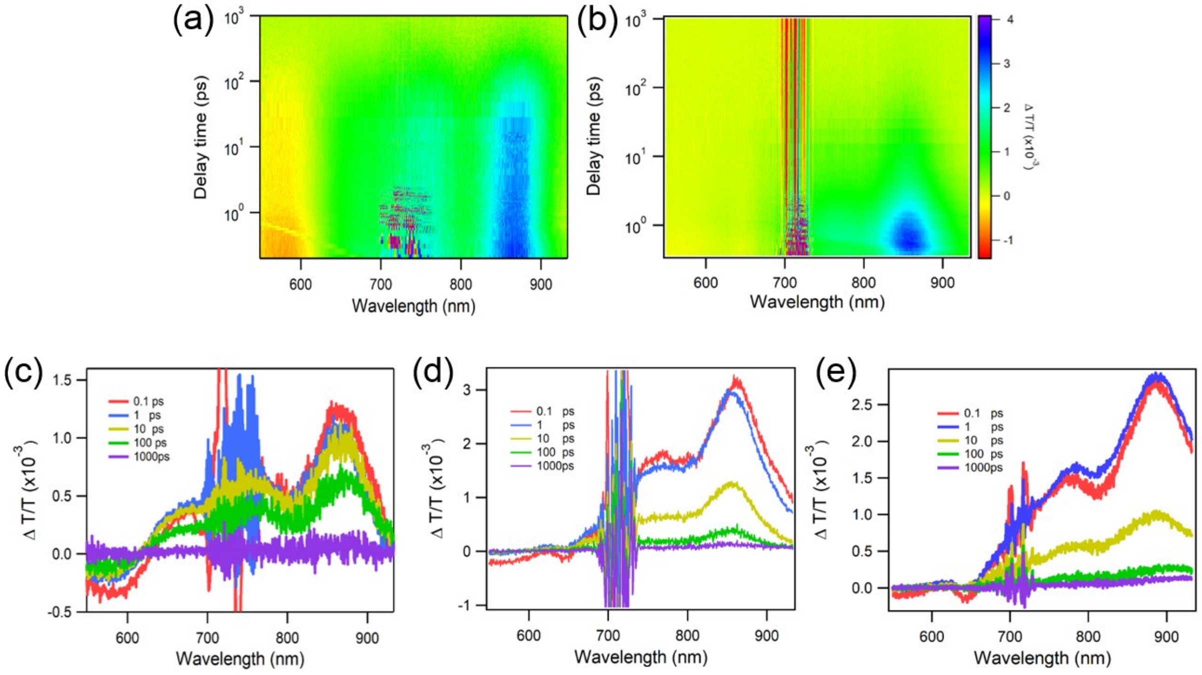

Fig. S5 Color plot of TA spectra of neat (a) H1 and (b) H2 under 750 nm excitation. Representative TA spectra (c) (d) (e) for H1, H2, H3 at indicated delay times.

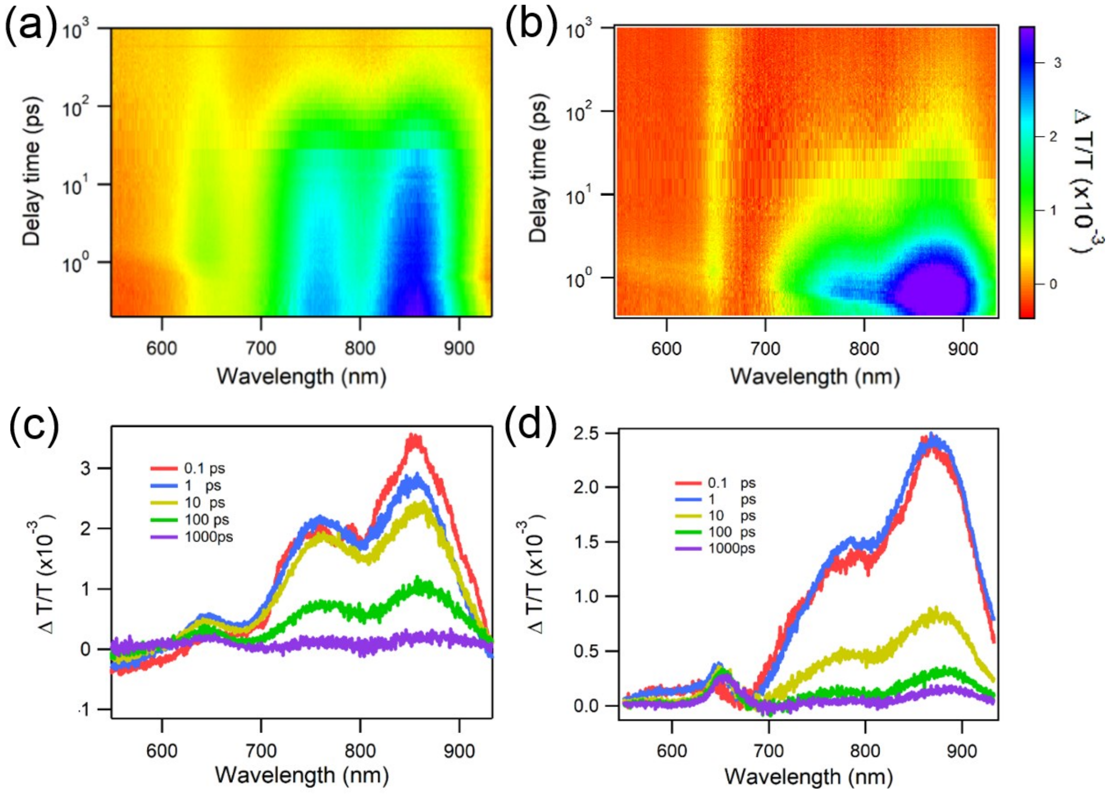

Fig. S6 Color plot of TA spectra of (a) PBDB-T:H1 and (b) PBDB-T:H2 blend film under 750 nm excitation. Representative TA spectra (c) (d) for PBDB-T:H1 and PBDB-T:H2 at indicated delay times.

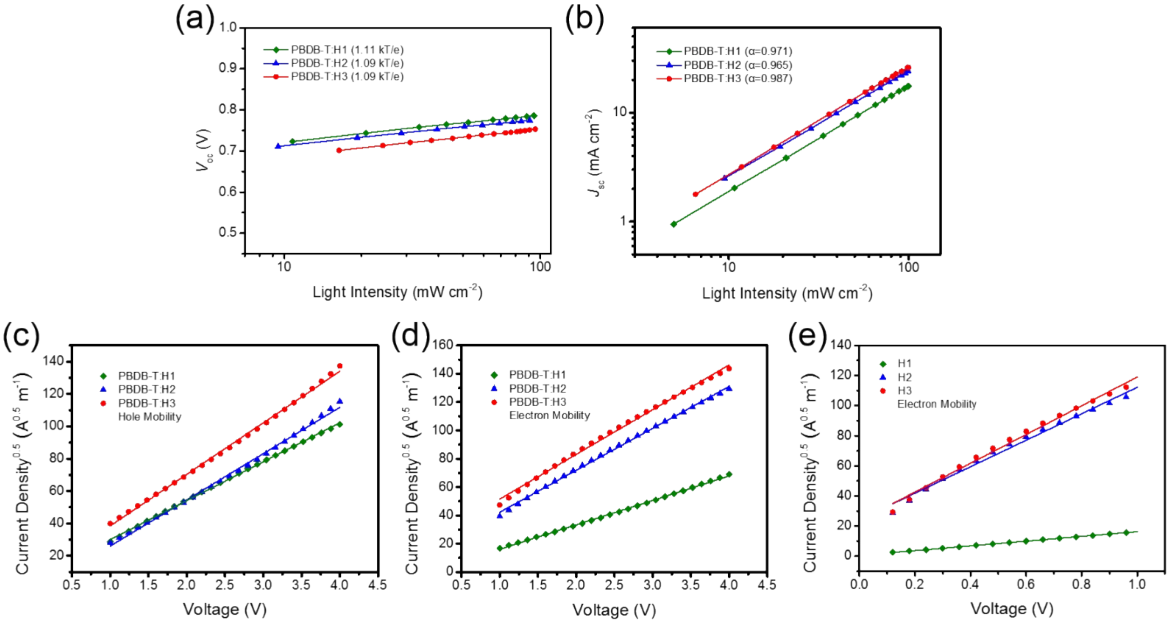

Fig. S7 (a) Dependencies of light intensity on V_{oc} of the optimized devices. (b) Dependencies of light intensity on J_{sc} of the optimized devices. (c) $J^{0.5}$-V curves of the hole-only devices from the three blend films. (d) $J^{0.5}$-V curves of the electron-only devices from the three blend films. (e) $J^{0.5}$-V curves of the electron-only devices from the three acceptor films.

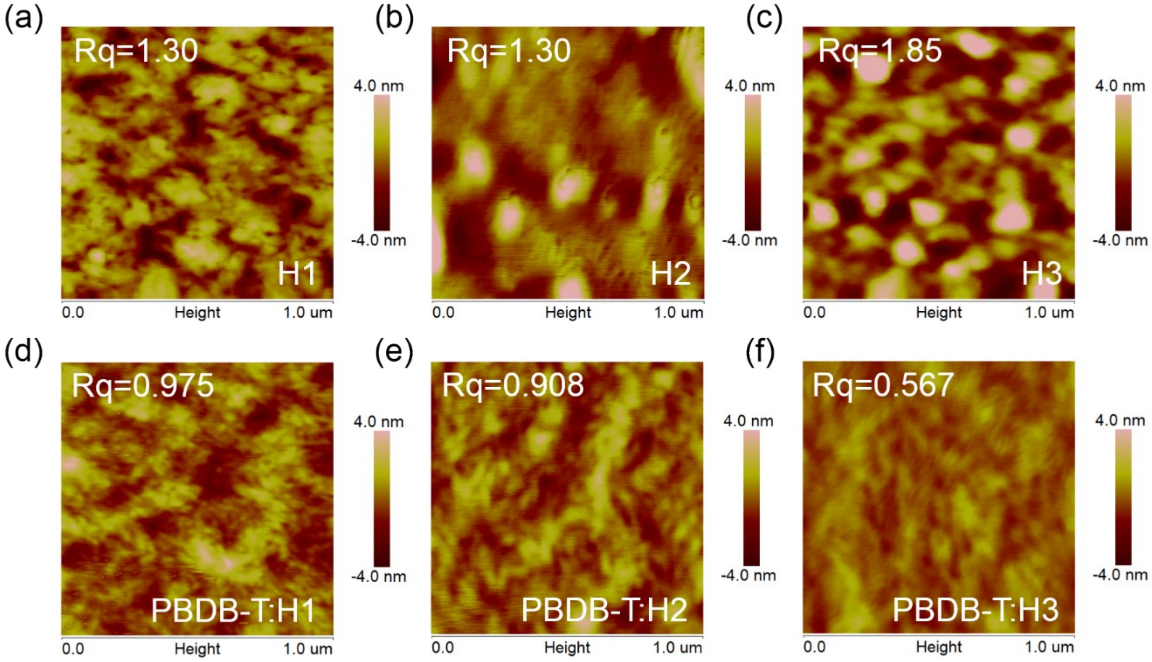

Fig. S8 AFM images of neat acceptor films and blend films.

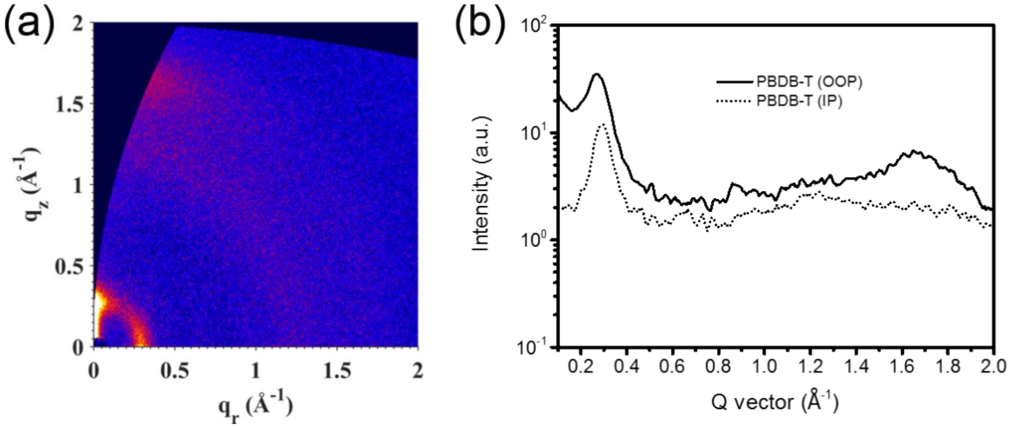

Fig. S9 2D GIWAXS image of PBDB-T and its intensity profiles.

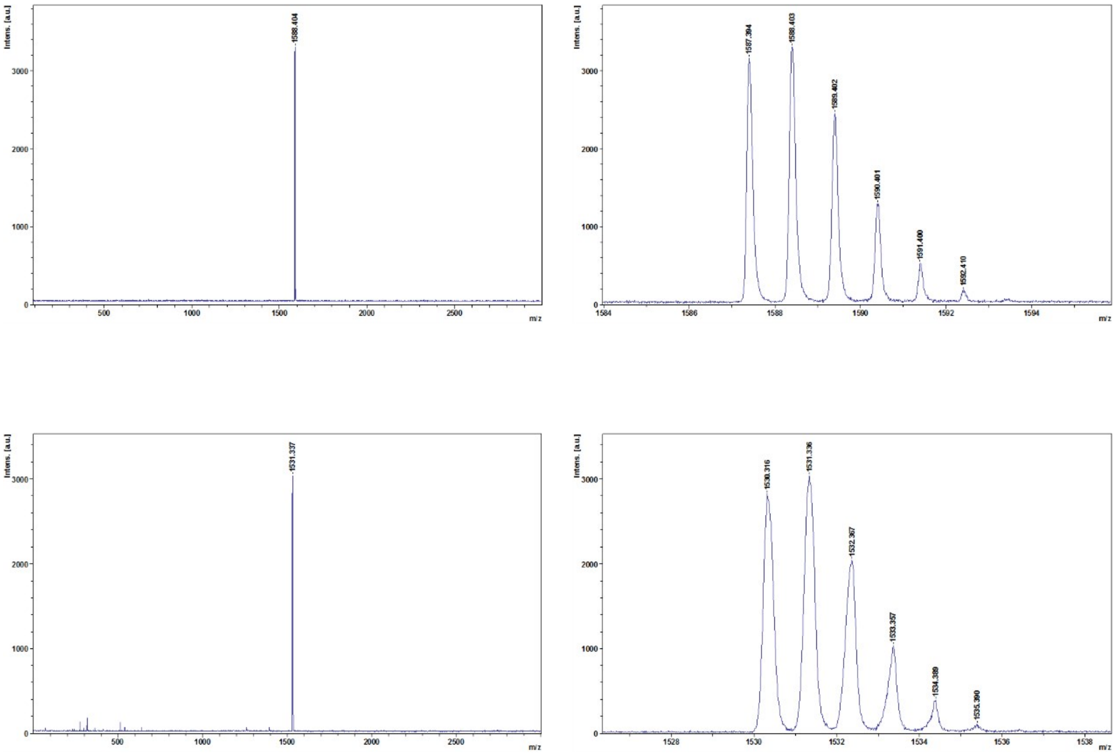

Fig. S10 The high resolution mass spectra of H1.

Fig. S11 The high resolution mass spectra of H2.

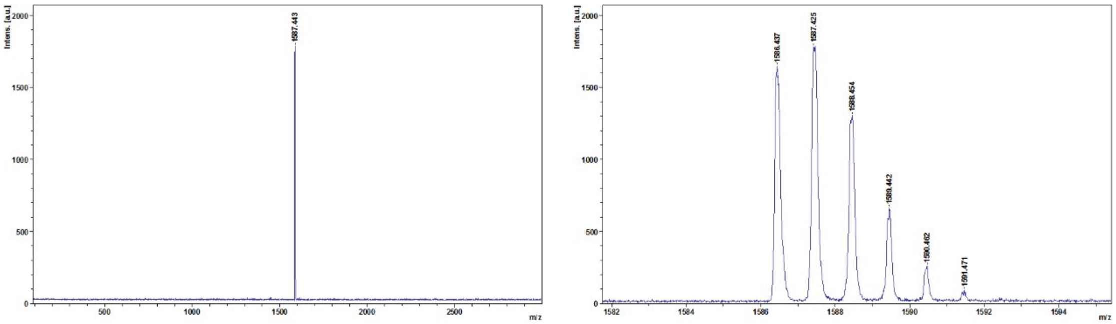

Fig. S12 The high resolution mass spectra of H3.

NMR Spectra

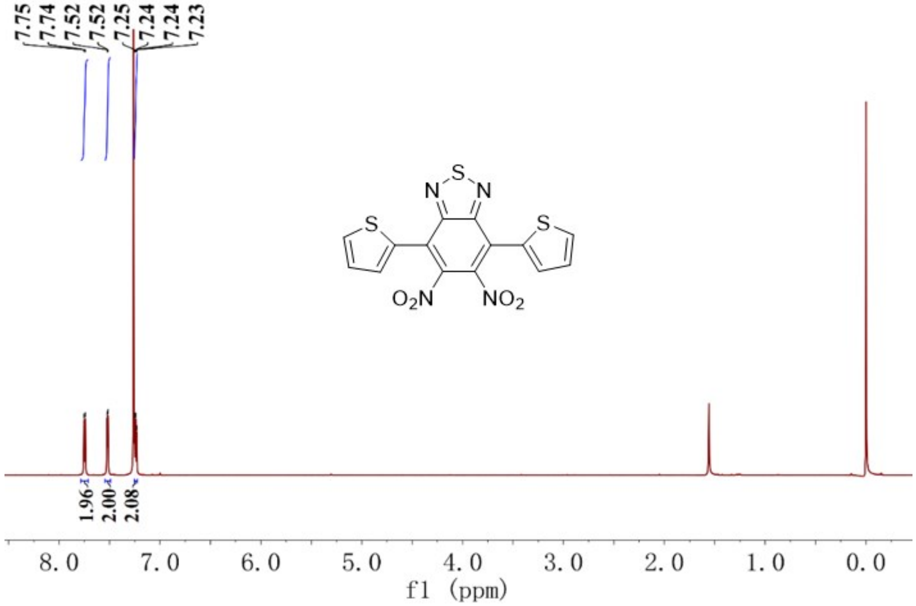

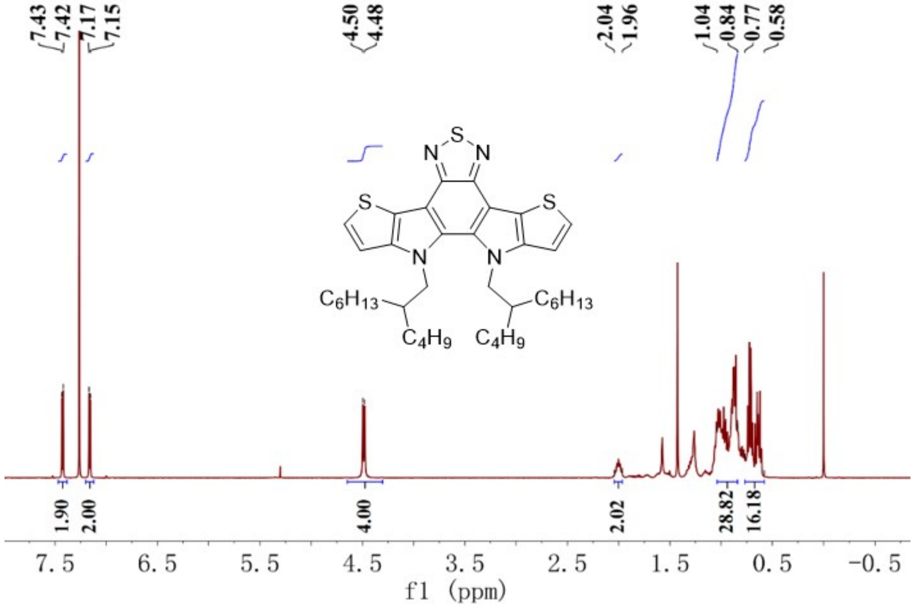
7.43
7.42
7.17
7.15
4.50
4.48
2.04
1.96
1.04
0.84
0.77
0.58
1.90
2.00
4.00
2.02
28.82
16.18
7.5
6.5
5.5
4.5
3.5
2.5
1.5
0.5
-0.5
f1 (ppm)
S
N
N
S
S
N
N
C6H13
C6H13
C4H9
C4H9

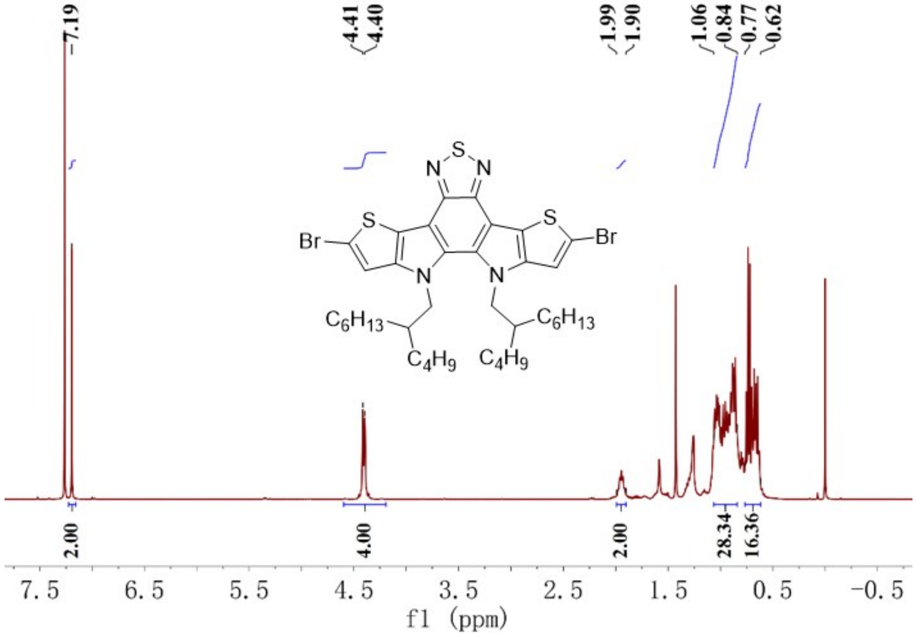
7.19
4.41
4.40
1.99
1.90
1.06
0.84
0.77
0.62
2.00
4.00
2.00
28.34
16.36
7.5
6.5
5.5
4.5
3.5
2.5
1.5
0.5
-0.5
f1 (ppm)
S
N
N
Br
S
S
Br
N
N
C6H13
C6H13
C4H9
C4H9

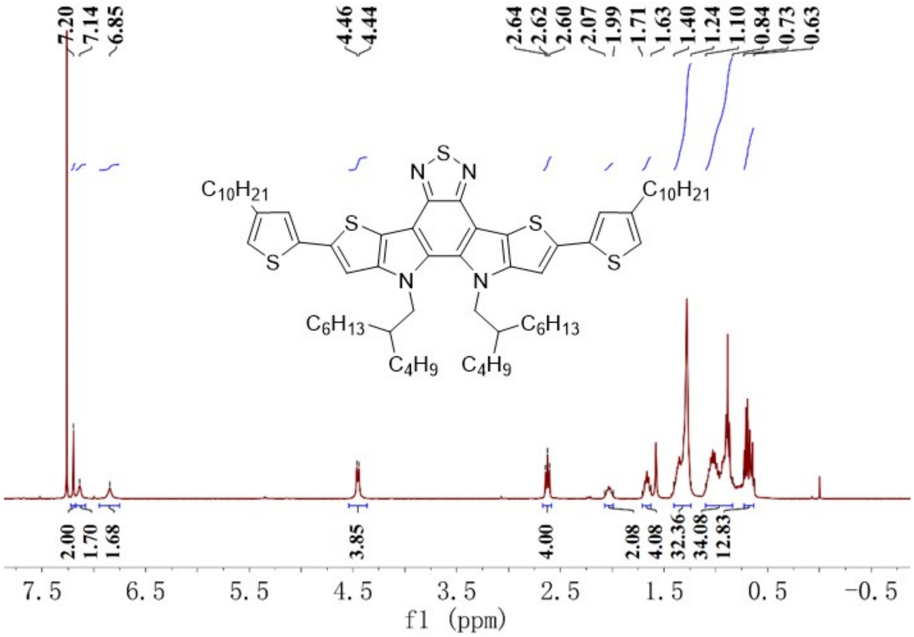
7.20
7.14
6.85
4.46
4.44
2.64
2.62
2.60
2.07
1.99
1.71
1.63
1.40
1.24
1.10
0.84
0.73
0.63
N
S
N
$C_{10}H_{21}$
S
S
S
S
N
N
$C_{10}H_{21}$
C_6H_{13}
C_6H_{13}
C_4H_9
C_4H_9
2.00
1.70
1.68
3.85
4.00
2.08
4.08
32.36
34.08
12.83
7.5
6.5
5.5
4.5
3.5
2.5
1.5
0.5
-0.5
f1 (ppm)

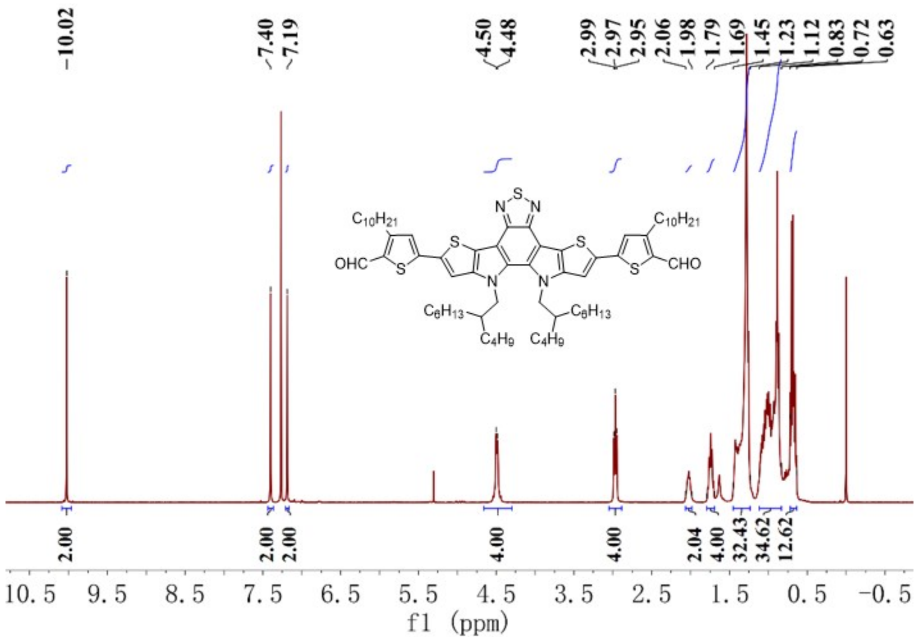
10.02
7.40
7.19
4.50
4.48
2.99
2.97
2.95
2.06
1.98
1.79
1.69
1.45
1.23
1.12
0.83
0.72
0.63
$C_{10}H_{21}$
$C_{10}H_{21}$
N
S
N
S
S
OHC
S
S
CHO
N
N
C_6H_{13}
C_6H_{13}
C_4H_9
C_4H_9
2.00
2.00
2.00
4.00
4.00
2.04
4.00
32.43
34.62
12.62
10.5
9.5
8.5
7.5
6.5
5.5
4.5
3.5
2.5
1.5
0.5
-0.5
f1 (ppm)

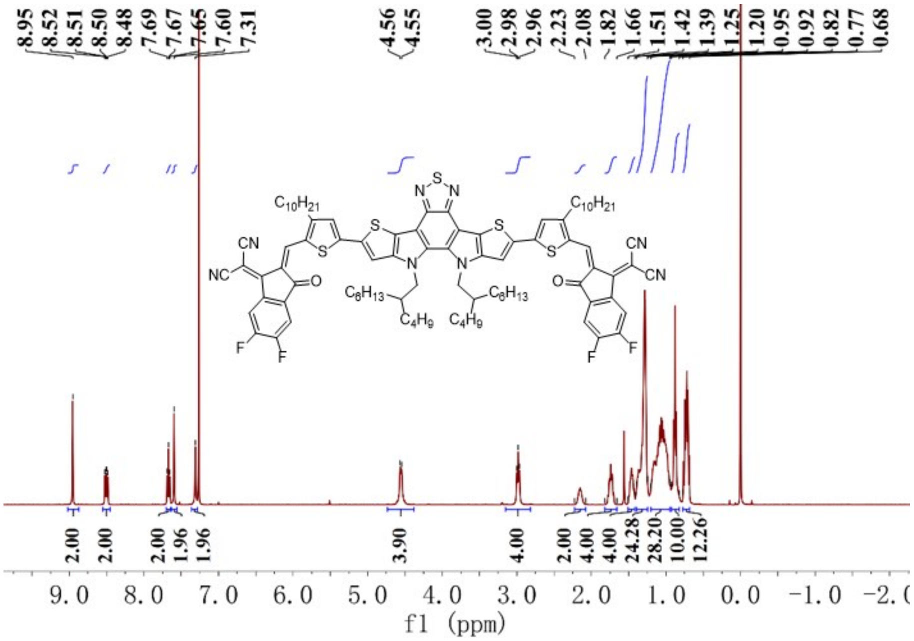
8.95
8.52
8.51
8.50
8.48
7.69
7.67
7.65
7.60
7.31
4.56
4.55
3.00
2.98
2.96
2.23
2.08
1.82
1.66
1.51
1.42
1.39
1.25
1.20
0.95
0.92
0.82
0.77
0.68
$C_{10}H_{21}$
$C_{10}H_{21}$
N
S
N
CN
CN
NC
S
S
S
S
CN
O
N
N
O
C_6H_{13}
C_6H_{13}
C_4H_9
C_4H_9
F
F
F
F
2.00
2.00
2.00
1.96
1.96
3.90
4.00
2.00
4.00
4.00
24.28
28.20
10.00
12.26
9.0
8.0
7.0
6.0
5.0
4.0
3.0
2.0
1.0
0.0
-1.0
-2.
f1 (ppm)

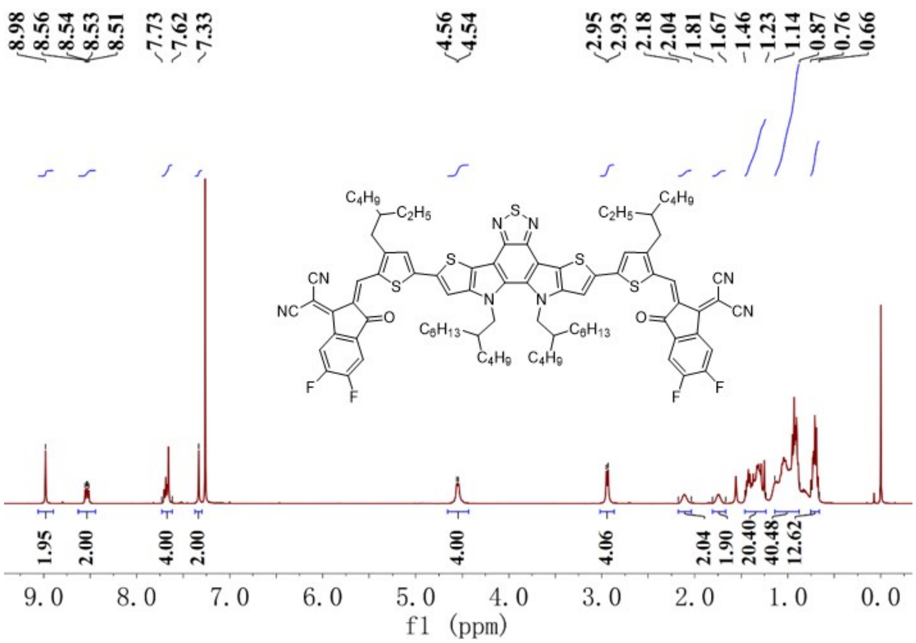
8.98
8.56
8.54
8.53
8.51
7.73
7.62
7.33
4.56
4.54
2.95
2.93
2.18
2.04
1.81
1.67
1.46
1.23
1.14
0.87
0.76
0.66
C4H9
C2H5
N
S
N
CN
NC
O
C6H13
F
1.95
2.00
4.00
2.00
4.00
4.06
2.04
1.90
20.40
40.48
12.62
9.0
8.0
7.0
6.0
5.0
4.0
3.0
2.0
1.0
0.0
f1 (ppm)

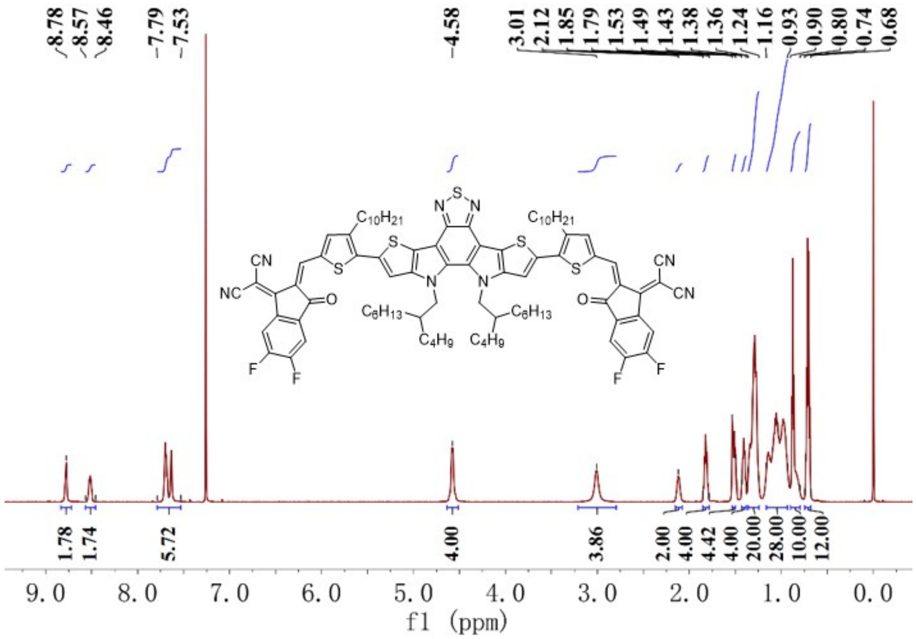
8.78
8.57
8.46
7.79
7.53
4.58
3.01
2.12
1.85
1.79
1.53
1.49
1.43
1.38
1.36
1.24
1.16
0.93
0.90
0.80
0.74
0.68
C10H21
N
S
N
CN
NC
O
C6H13
C4H9
F
1.78
1.74
5.72
4.00
3.86
2.00
4.00
4.42
4.00
20.00
28.00
10.00
12.00
9.0
8.0
7.0
6.0
5.0
4.0
3.0
2.0
1.0
0.0
f1 (ppm)

Table S1 Summary of Device Parameters of This Work and Reported References.

Active layers	V_{oc}	J_{sc}	FF	PCE	E_g[a]	Edge[a]	ref
PTB7-Th:CO1-4F	0.64	24.8	0.64	10.2	1.2	1033	1
PTB7-Th:CTIC-4F	0.7	23.4	0.64	10.5	1.3	954	1
PTB7-Th:IEICO-4Cl	0.727	22.8	0.62	10.3	1.227	1010	2
PTB7-Th:3TT-CIC	0.65	26.67	0.69	11.96	1.23	1008	3
PTB7-Th:3TT-OCIC	0.68	26.49	0.69	12.43	1.29	961	3
PBDTTT-EFT:IEICO-4F	0.74	22.8	0.59	10	1.24	1000	4
PTB7-Th:DTPC-DFIC	0.76	21.92	0.61	10.2	1.21	1025	5
PTB7-Th:F8IC	0.64	25.12	0.68	10.9	1.27	976	6
PTB7-Th:T2	0.67	22.65	0.66	10.1	1.28	968	7
PTB7-Th:COi8DFIC	0.68	26.12	0.68	12.16	1.26	984	8
PBDB-T:IXIC-2Cl	0.73	23.6	0.71	12.2	1.298	955	9
PBDB-T:IXIC-4Cl	0.69	22.9	0.71	11.2	1.25	990	9
PTB7-Th:IEICO-4F	0.712	27.3	0.66	12.8	1.24	1000	10
PBDB-T:H2	0.781	24.4	0.69	13.15	1.22	1016	This work
PBDB-T:H3	0.757	25.84	0.70	13.75	1.22	1016	This work

[a] Obtained from the given values from the reference.

Table S2 Detailed Data of GIWAXS Characterization.

Samples		(100)		(010)	
		Position/Å^{-1}	d-spacing/Å	Position/Å^{-1}	d-spacing/Å
PBDB-T	q_r	0.295	21.3		

Table S3 Photovoltaic parameters of OSCs based on different polymer donors.

Active Layer	V_{oc} (V)	J_{sc} (mA cm^{-2})	FF	PCE (%)
PCE10:H3	0.727	23.38	0.62	10.56
PBDB-T:H3	0.757	25.84	0.70	13.75
PBDB-TF:H3	0.813	16.99	0.60	8.22

H1	q_z	0.270	23.3	1.65	3.81
	q_r			1.82	3.45
	q_z	0.305 0.635	20.6 9.89		
H2	q_r	0.385	16.3	1.80	3.49
	q_z	0.335 0.680	18.8 9.24	1.77	3.56
H3	q_r	0.272 0.375	23.1 16.8		
	q_z			1.80	3.50
PBDB-T:H1	q_r	0.305	20.6		
	q_z	0.290	21.7	1.76	3.57
PBDB-T:H2	q_r	0.315	20.0		
	q_z	0.280	22.4	1.76	3.57
PBDB-T:H3	q_r	0.300	20.9		
	q_z	0.260	24.2	1.77	3.55

REFERENCES

1 J. Lee, S.-J. Ko, H. Lee, J. Huang, Z. Zhu, M. Seifrid, J. Vollbrecht, V. V. Brus, A. Karki, H. Wang, K. Cho, T.-Q. Nguyen and G. C. Bazan, *ACS Energy Lett.*, 2019, **4**, 1401-1409.

2 Y. Cui, C. Yang, H. Yao, J. Zhu, Y. Wang, G. Jia, F. Gao and J. Hou, *Adv. Mater.*, 2017, **29**, 1703080.

3 H. H. Gao, Y. Sun, Y. Cai, X. Wan, L. Meng, X. Ke, S. Li, Y. Zhang, R. Xia, N. Zheng, Z. Xie, C. Li, M. Zhang, H. L. Yip, Y. Cao and Y. Chen, *Adv. Energy Mater.*, 2019, **9**, 1901024.

4 H. Yao, Y. Cui, R. Yu, B. Gao, H. Zhang and J. Hou, *Angew. Chem. Int. Ed.*, 2017, **56**, 3045-3049.
5 Z. Yao, X. Liao, K. Gao, F. Lin, X. Xu, X. Shi, L. Zuo, F. Liu, Y. Chen and A. K. Jen, *J. Am. Chem. Soc.*, 2018, **140**, 2054-2057.
6 S. Dai, T. Li, W. Wang, Y. Xiao, T. K. Lau, Z. Li, K. Liu, X. Lu and X. Zhan, *Adv. Mater.*, 2018, **30**, 1706571.
7 F. X. Chen, J. Q. Xu, Z. X. Liu, M. Chen, R. Xia, Y. Yang, T. K. Lau, Y. Zhang, X. Lu, H. L. Yip, A. K. Jen, H. Chen and C. Z. Li, *Adv. Mater.*, 2018, **30**, 1803769.
8 Z. Xiao, X. Jia, D. Li, S. Wang, X. Geng, F. Liu, J. Chen, S. Yang, T. P. Russell and L. Ding, *Sci. Bull.*, 2017, **62**, 1494-1496.
9 Y. Chen, T. Liu, H. Hu, T. Ma, J. Y. L. Lai, J. Zhang, H. Ade and H. Yan, *Adv. Energy Mater.*, 2018, **8**, 1801203.
10 X. Song, N. Gasparini, L. Ye, H. Yao, J. Hou, H. Ade and D. Baran, *ACS Energy Lett.*, 2018, **3**, 669-676.